**Proceedings of ASME Turbo Expo 2011**
**GT2011**
**June 6-10, 2011, Vancouver, British Columbia, Canada**

**GT2011-45597**

# INTERVAL ANALYSIS METHOD FOR ROTORDYNAMICS WITH UNCERTAIN PARAMETERS

**Ma Yanhong[1], Cao Peng[1], Wang Jun[1,2], Chen Meng[1], Hong Jie[1]**
1. School of Jet Propulsion, Beijing University of Aero. and Astro.
No.37 Xueyuan Rd. Haidian District, Beijing, China, 100191
2. Shenyang Aeroengine Research Institute
No.1 Wanlian Rd. Shenhe District, Shenyang, China, 110015

## ABSTRACT

The support stiffness and connecting structure stiffness which has significant effect on rotordynamics change with different assembly conditions and operating conditions. For example, the squeeze film stiffness changes with different film force, and the elastic support stiffness changes with different temperatures. These parameters are "uncertain but bounded", in another word, the distributions of the parameters are unknown, but the intervals of the uncertain parameters are always got easier.

An interval analysis method, which solves the rotordynamics with these uncertain parameters, is presented. Based on interval mathematics and perturbation method, interval analysis method simplifies the uncertain parameters to interval vectors so that it can get the intervals within which the rotordynamics varies when less information of structure is known. The interval analysis method is efficient under the condition that probability approach cannot work because of small samples and spare statistics characteristics. The formulation of natural frequencies of rotor using interval perturbation analysis method is formulated. A numerical example of comparison between interval perturbation method analysis and monotonic method is given. The rotordynamic analysis of a turbofan rotor is performed with this method, and the test data validates the numerical results.

## 1. INTRODUCTION

Rotordynamic analysis is very important for the design of aero-engines. Nowadays the finite element method is becoming increasingly popular in analyzing complicated rotor systems, as it is capable of predicting the static and dynamic behavior of the structure based on its geometry and material characteristics, the applied loads and constraints.

However, it is often very difficult to define a reliable FE model of the rotor system, especially when a number of physical properties are uncertain. In real life, many components of a rotor system are subject to uncertainty. There are three types of uncertain in the rotor system. The first type is probabilistic uncertain, and in this case the uncertain parameters are described as random variables with known probability distributions. The second type is the fuzzy uncertain, which is non-probabilistic uncertain because sufficiently reliable stochastic data are not available. In fuzzy theory, the uncertainty is interpreted as the designer and analysis choice to use a particular value for the uncertain variable, if a preference function is used to describe the desirability of using different values within the same range. The last type is the interval uncertain, in which parameters are "uncertain but bounded". It can be seen that when information about uncertain variables in the form of a preference or probability function is not available, interval analysis can be used most conveniently.

If the uncertainties can affect the dynamics of the rotor system greatly, the validation of a structure with the FEM can only be reliable when taking the uncertainties into account. Many papers focus on the probabilistic uncertain of rotor systems, from random structures to random external forces [1-2], and there are also some papers on the rotor system with fuzzy uncertainties [3]. But there is rarely any work on the interval analysis of rotordynamics.

In this paper, an interval analysis method, which solves the rotordynamics with these uncertain parameters, is presented. Based on interval mathematics and perturbation method, interval analysis method simplifies the uncertain parameters to interval vectors so that it can get the intervals within which the rotordynamics varies when less information of structure is known. The interval analysis method is efficient under the condition that probability approach cannot work because of small samples and spare statistics characteristics. The formulation of natural frequencies of rotor considering gyroscopic moments using interval perturbation analysis method is formulated. A numerical example of comparison between interval perturbation method analysis and monotonic method is given. The rotordynamic analysis of a turbofan rotor is performed with this method, and the test data validates the numerical results.

## 2. UNCERTAINS IN ROTOR SYSTEM AND INTERVAL ANALYSIS METHOD

### 2.1 Uncertainties in rotor system

Due to the randomness in material and geometric properties, or varying operation circumstance in rotor systems, uncertainties exist widely in the rotor-bearing systems. The exact actions such as bearing loads and rotational speeds are all subject to variations. The lubricant properties such as density and viscosity vary with the oil temperature. The performance of components such as bearings and shafts vary during their lifetimes because of wear and changes in operating conditions. Among these uncertainties, the support stiffness and connecting structure stiffness [4] are significant parameters that affect the rotor critical speed and vibration modes.

As shown in Fig. 1, the support stiffness generally consists of three parts: the support structure stiffness $K_{Structure}$, the stiffness of squeeze film damper ($K_{SFD}$) and the stiffness of bearing ($K_{brg}$). $K_{Structure}$ and $K_{SFD}$ change with different temperature and loads, and $K_{brg}$ changes with temperature, assembly state and loads.

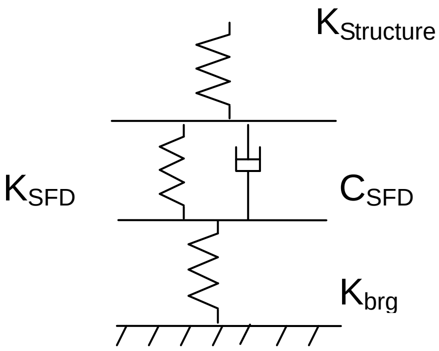


**Fig. 1 The composition of support stiffness**

The connecting structures in aero-engine rotors such as spline joint structures and bolted joint structures (shown in Fig.2) were employed to hold two or more parts with different materials together to form an integrated rotor frame in a mechanical structure, in which rigidity and a mating part contact are the two primary characteristics. The stiffness of connecting structures changes with different working conditions (temperature, rotating speed) and initial assembly statement.

These parameters are typical “uncertain but bounded” ones, in another word, the distributions of the parameters are unknown, but the intervals of the uncertain parameters are always got easier. An interval method [5-6] is introduced to analyze the effect of these parameters on rotordynamics.

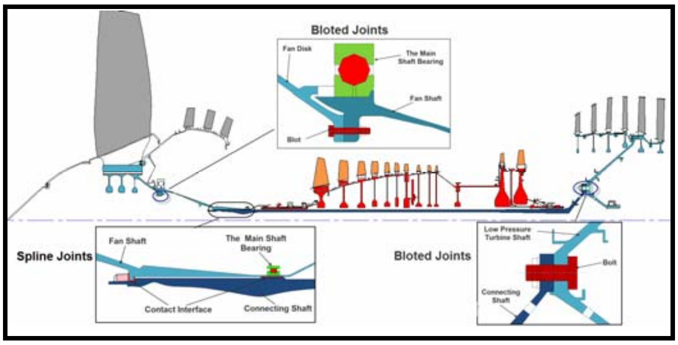


**Fig.2 Connecting structures of an aero-engine rotor**

### 2.2 Interval analysis method

The equation of motion of the rotor includes the structural parameters, such as mass, connecting stiffness and supporting stiffness etc., which can be represented as

$$a = (a_1, a_2, \cdots a_m)^T$$

In the deterministic rotordynamic analysis, only the deterministic value or nominal value $a^c$ of these structural parameters is considered. However, in the uncertain rotordynamic analysis, the influence of the uncertainties of structural parameters on rotordynamics also needs to be considered.

In practice, usually no sufficient information on uncertainty can be obtained so that it is difficult to determine their statistical characteristics. Nevertheless, the bounds of uncertain parameters often can be defined easily. They can be described by interval notation as:

$$a_i \in a_i^I = [\underline{a_i}, \overline{a_i}] = [a_i^c - \Delta a_i, a_i^c + \Delta a_i] = a_i^c + \Delta a_i^I \quad (1)$$

where

$$\Delta a_i^I = [-\Delta a, \Delta a] \quad (2)$$

Then the interval uncertain parameters can be described as

$$\begin{cases} a = a^c + \delta a, & |\delta a| \le \Delta a \\ a_i = a_i^c + \delta a_i, & |\delta a_i| \le \Delta a_i, i = 1,2,\cdots,m \end{cases} \quad (3)$$

Let us consider the differential equation of motion of rotor systems with $n$ degrees of freedom

$$M\ddot{z} + (C+G)\dot{z} + Kz = 0 \quad (4)$$

Where $M = (m_{ij})$ is the mass matrix, $C = (c_{ij})$ is the damping matrix, $G = (g_{ij})$ is the gyroscopic matrix, $K = (k_{ij})$ is the stiffness matrix, respectively. $M = (m_{ij})$ is the positive definite matrix. $C = (c_{ij})$ and $K = (k_{ij})$ are the positive semi-definite matrices. $G = (g_{ij})$ is the anti-symmetric matrix.

By state transformation, Eq. (4) can be written in the form

$$B\dot{x} - Ax = 0 \quad (5)$$

Where

$$x = [\begin{matrix} \dot{z} \\ z \end{matrix}], A = \begin{bmatrix} M & 0 \\ 0 & -K \end{bmatrix}, \quad B = \begin{bmatrix} 0 & M \\ M & C+G \end{bmatrix} \quad (6)$$

in which A is $2n \times 2n$-dimensional real symmetric non-positive definite matrix, and B is $2n\times 2n$-dimensional dissymmetry matrix.

The generalized complex eigenvalue problem corresponding to Eq. (6) has the following form:

$$Au = \lambda Bu \tag{7}$$

$$v^T A = \lambda v^T B \tag{8}$$

Where λ is the complex eigenvalue, $u = [\begin{smallmatrix}\lambda\phi \\ \phi\end{smallmatrix}]$ is the $2n$ complex right eigenvector， v is the $2n$ complex left eigenvector, ϕ is the $n$ complex eigenvector.

The natural frequency analysis of the rotor system with uncertain parameters can be described as Eq. (4) with constraint Eq. (9).

$$\underline{m_{ij}} \le m_{ij} \le \overline{m_{ij}}\ ,\quad \underline{c_{ij}} \le c_{ij} \le \overline{c_{ij}}\ ,$$

$$\underline{g_{ij}} \le g_{ij} \le \overline{g_{ij}}\ ,\quad \underline{k_{ij}} \le k_{ij} \le \overline{k_{ij}} \tag{9}$$

Based on Eq. (5), Eq. (9) can be written in the form

$$\underline{A} \le A \le \overline{A}\ ,\quad \underline{B} \le B \le \overline{B} \tag{10}$$

Where

$$\underline{A} = \begin{bmatrix} (\underline{m_{ij}}) & 0 \\ 0 & (-\overline{k_{ij}}) \end{bmatrix}, \overline{A} = \begin{bmatrix} (\overline{m_{ij}}) & 0 \\ 0 & (-\underline{k_{ij}}) \end{bmatrix},$$

$$\underline{B} = \begin{bmatrix} 0 & (\underline{m_{ij}}) \\ (\underline{m_{ij}}) & (\underline{c_{ij}} + \underline{g_{ij}}) \end{bmatrix}, \overline{B} = \begin{bmatrix} 0 & (\overline{m_{ij}}) \\ (\overline{m_{ij}}) & (\overline{c_{ij}} + \overline{g_{ij}}) \end{bmatrix} \tag{11}$$

According to the formulation of interval matrices, Eq. (10) can be written as

$$A \in A^I\ ,\quad B \in B^I \tag{12}$$

Then Eq. (7) and Eq. (8) can be written as

$$A^I u = \lambda B^I u \tag{13}$$

$$v^T A^I = \lambda v^T B^I \tag{14}$$

Based on Eq.(1), Eq.(13) can be written as

$$(A^c + \Delta A^I)u = \lambda (B^c + \Delta B^I)u \tag{15}$$

If small changes are introduced to matrices A and B:

$$A = A^c + \delta A\ ,\quad B = B^c + \delta B \tag{16}$$

Where $A^c$ and $B^c$ are the unperturbed matrix pair, and $\delta A$ and $\delta B$ are the matrix pair representing the small changes from $A^c$ and $B^c$. We shall refer to A and B as the perturbed matrix pair. The perturbed generalized eigenvalue problem can be written in the form

$$(A^c + \delta A)u = \lambda (B^c + \delta B)u \tag{17}$$

where $-\Delta A \le \delta A \le \Delta A$ , $-\Delta B \le \delta B \le \Delta B$ (18)

One can obtain the expression of the first perturbation eigenvalues for the perturbed matrix pair $A = A^c + \delta A$ and $B = B^c + \delta B$ as follows:

$$\lambda_i = \lambda_{ir}^I + \sqrt{-1}\lambda_{iy}^I = \lambda_{ci} + \delta\lambda_i^I\ ,\ i = 1,2,\cdots,n \tag{19}$$

Where

$$\begin{aligned}\lambda_{ir}^I = \lambda_{cir} &+ (v_{cir}^T \Delta A^I u_{cir} - v_{ciy}^T \Delta A^I u_{ciy}) \\ &- \lambda_{cir}(v_{cir}^T \Delta B^I u_{cir} - v_{ciy}^T \Delta B^I u_{ciy}) \\ &+ \lambda_{ciy}(v_{cir}^T \Delta B^I u_{ciy} + v_{ciy}^T \Delta B^I u_{cir})\end{aligned} \tag{20}$$

$$\begin{aligned}\lambda_{iy}^I = \lambda_{ciy} &+ (v_{cir}^T \Delta A^I u_{ciy} + v_{ciy}^T \Delta A^I u_{cir}) \\ &- \lambda_{ciy}(v_{cir}^T \Delta B^I u_{cir} - v_{ciy}^T \Delta B^I u_{ciy}) \\ &- \lambda_{cir}(v_{cir}^T \Delta B^I u_{ciy} + v_{ciy}^T \Delta B^I u_{cir})\end{aligned} \tag{21}$$

By the interval mathematics or interval analysis, Eq. (20) and Eq. (21) can be written in another form:

$$\lambda_{ir}^I = [\lambda_{cir} - \Delta\lambda_{ir}, \lambda_{cir} + \Delta\lambda_{ir}] \quad i = 1,2,\cdots,n \tag{22}$$

$$\lambda_{iy}^I = [\lambda_{ciy} - \Delta\lambda_{iy}, \lambda_{ciy} + \Delta\lambda_{iy}] \quad i = 1,2,\cdots,n \tag{23}$$

Where

$$\Delta\lambda_{ir} = \begin{vmatrix} v_{cir}^T \Delta A^I u_{cir} - v_{ciy}^T \Delta A^I u_{ciy} \\ -\lambda_{cir}(v_{cir}^T \Delta B^I u_{cir} - v_{ciy}^T \Delta B^I u_{ciy}) \\ +\lambda_{ciy}(v_{cir}^T \Delta B^I u_{ciy} + v_{ciy}^T \Delta B^I u_{cir}) \end{vmatrix} \tag{24}$$

$$\Delta\lambda_{iy} = \begin{vmatrix} v_{cir}^T \Delta A^I u_{ciy} + v_{ciy}^T \Delta A^I u_{cir} \\ -\lambda_{ciy}(v_{cir}^T \Delta B^I u_{cir} - v_{ciy}^T \Delta B^I u_{ciy}) \\ -\lambda_{cir}(v_{cir}^T \Delta B^I u_{ciy} + v_{ciy}^T \Delta B^I u_{cir}) \end{vmatrix} \tag{25}$$

In Eqs.(24) and (25), the eigenvalues $\lambda_{ci} = \lambda_{cir} + \sqrt{-1}\lambda_{ciy}$, $i = 1,2,\cdots,n$ and the eigenvectors $v_{ci} = v_{cir} + \sqrt{-1}v_{ciy}$ , $i = 1,2,\cdots,n$ and $u_{ci} = u_{cir} + \sqrt{-1}u_{ciy}$, $i = 1,2,\cdots,n$ satisfy

$$A^c u_{ci} = \lambda_{ci} B^c u_{ci} \tag{26}$$

$$v_{ci}^T A^c = \lambda_{ci} v_{ci}^T B^c \tag{27}$$

$$v_{ci}^T B^c u_{ci} = 1 \tag{28}$$

Obviously, from Eqs. (22) and (23), we can see that we only need to solve two generalized eigenvalue problems and compute four expressions, then all interval eigenvalues of the interval matrix can be determined. Thus, the presented method is very practical.

According to Eqs. (23) and (25), the interval natural frequencies of the rotor system can be written as

$$f_i^I = [f_{ci} - \Delta f_i, f_{ci} + \Delta f_i] \quad i = 1,2,\cdots,n \tag{29}$$

Where $f_{ci} = \lambda_{ci}/2\pi$, and $\Delta f_i = \Delta\lambda_{iy}/2\pi$.

**2.3 Summary of monotonic method**

If $f(x_1, x_2, \cdots x_n)$ is a monotone function of interval parameters $x_i, i = 1,2,\cdots,n$, then the bound of $f$ can be captured from the combination of all the import parameters. Let

$$x_i = [x_i^{(1)}, x_i^{(2)}] = [\underline{x_i}, \overline{x_i}], \quad i = 1,2,\cdots,n \qquad (30)$$

Then all the possible extreme value of $f$ can be written as

$$f_r = f(x_1^{(i)}, x_2^{(j)}, \cdots x_n^{(k)}) \qquad (31)$$

Where $i = 1,2$, $j = 1,2$, $k = 1,2$, $r = 1,2,\cdots,2^n$.

Finally the bound of $f(x_1, x_2, \cdots x_n)$ is

$$f = [\underline{f}, \overline{f}] = [\min_{r=1,2,\cdots 2^n}(f_r), \max_{r=1,2,\cdots 2^n}(f_r)] \qquad (32)$$

This monotonic method can calculate the interval variation bound of the response function accurately, but the calculation efficiency will decrease with the increase of the number of uncertain parameters.

## 3. NUMERICAL EXAMPLE

In this section, a single-disk rotor is modeled by beam element with interval parameters, and natural frequency (complex eigenvalue) analysis is performed with interval perturbation method.

The model of the rotor is shown in Fig.3. The length of the shaft is *L=0.75m*, the diameter *R=0.06m*, *L1=0.1m*, *L2=L3=0.15m*. The rotor is modeled with 10 beam elements and 1 mass element. In this example it is assumed that the stiffness coefficient of support 2 $K_2$, the density $\rho$ and Elastic modulus $E$ are uncertain-but-bounded variables, and the interval stiffness of support 2 is taken as $K_2 = [K_2^c - \beta K_2^c, K_2^c + \beta K_2^c]$, the interval density $\rho = [\rho^c - \beta\rho^c, \rho^c + \beta\rho^c]$, and interval Elastic modulus $E = [E^c - \beta E^c, E^c + \beta E^c]$, where $K_2^C = 3.0e6N/m$, $\rho^C = 7.8e03Kg/m^3$, and $E^C = 200GPa$. Other quantities are deterministic, in which the mass of the disk is taken as $m=20Kg$, and the polar moment of inertia $I_p = 0.144kg \cdot m^2$, the stiffness coefficient of support 1 $K_1 = 1.0e8N/m$, the rotating speed $\omega = 6{,}000rpm$.

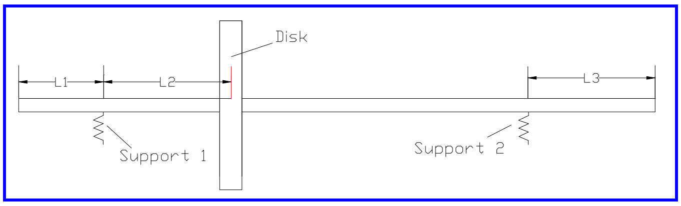


**Fig.3 The single-disk rotor model**

The natural frequencies computed by the perturbation method are listed in Table **1** when the variable parameter $\beta$ is taken as $\beta$=0.05. In the tables $k$ is the number of modes; $f_i^c$ are the nominal frequencies, $\underline{f_i^p}$ and $\overline{f_i^p}$ are the lower bound and upper bound of the natural frequencies using the perturbation method, respectively. $\underline{f_i^a}$ and $\overline{f_i^a}$ are the accurate lower bound and upper bound of the natural frequencies calculated with the monotonic method of reference [7], because the lateral vibration frequencies are monotonic to support stiffness $K_2$, the density $\rho$ and elastic modulus $E$, respectively. The corresponding mode shapes of the frequencies are shown in Fig.4.

**Table 1. Lower and upper bounds of natural frequencies (Hz)**

| k | Mode shapes | $f_i^c$ | $\underline{f_i^p}$ | $\overline{f_i^p}$ | $\underline{f_i^a}$ | $\overline{f_i^a}$ |
|---|---|---|---|---|---|---|
| 1 | Fig.4 a | 93.656 | 89.616 | 97.695 | 89.667 | 97.751 |
| 2 | | 99.614 | 95.372 | 103.857 | 95.429 | 103.918 |
| 3 | Fig.4 b | 251.085 | 242.785 | 259.384 | 242.834 | 259.449 |
| 4 | | 251.191 | 242.967 | 259.415 | 243.027 | 259.492 |
| 5 | Fig.4 c | 581.948 | 566.751 | 597.144 | 567.004 | 597.423 |
| 6 | | 644.836 | 627.401 | 662.271 | 627.752 | 662.653 |

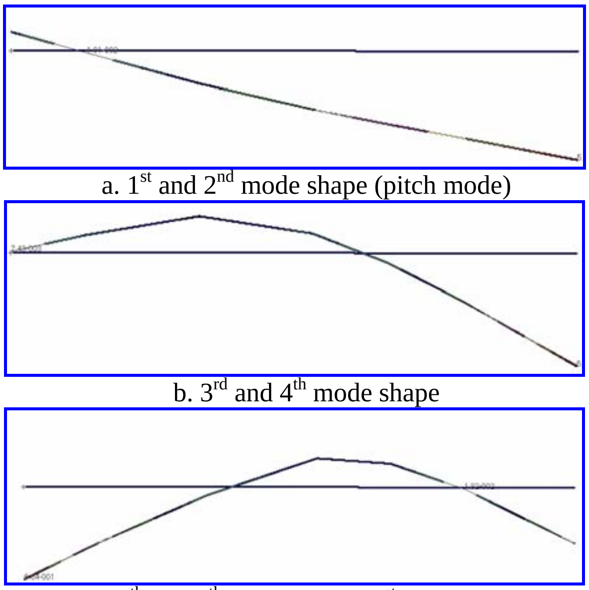

a. 1st and 2nd mode shape (pitch mode)

b. 3rd and 4th mode shape

c. 5th and 6th mode shape (1st bending)

**Fig.4 Mode shapes of the single-disk rotor**

From the results listed in Table 1 , we can see that there are very little difference between the maximum or upper bounds and the minimum or lower bounds on the natural frequencies yielded by the perturbation method and those produced by monotonic method. The separation margin is less than 0.05%.

Comparisons of the range curves of the natural frequencies of the system computed by the interval perturbation method and monotonic solution theorem when the variable parameter $\beta$ ranges from 0.0 to 0.2 are plotted in Fig.5 (a) – (c).

It can be seen from Fig.5 that when $\beta$ is less than 0.05, the natural frequencies calculated by interval perturbation method are the same as the accurate frequencies. When $\beta$ increases from 0.05 to 0.2, the natural frequencies calculated by interval perturbation method are very close to the accurate frequencies. The separation margin is less than 0.8%.

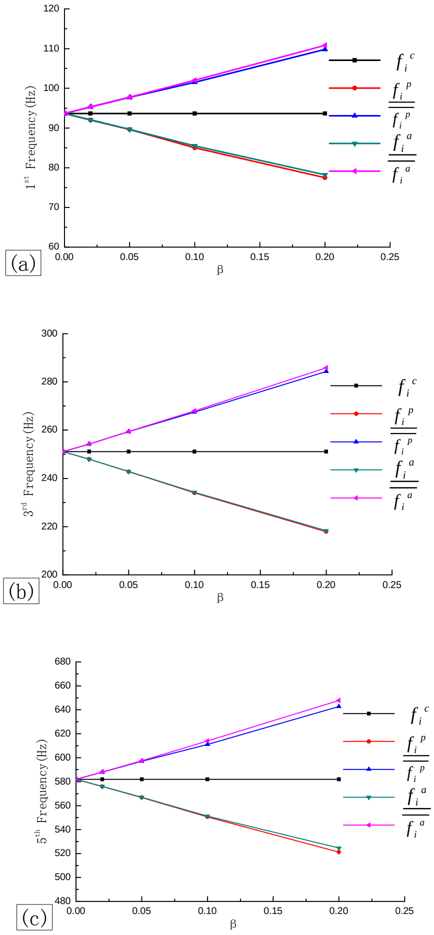


**Fig.5 Comparison of the region curves of natural frequencies yielded by the monotonic method and the interval perturbation method**

## 4. ROTORDYNAMIC ANALYSIS OF A TURBINE-FAN ROTOR

### 4.1 Numerical analysis

The subject rotor is a typical small turbine-fan rotor [8], including fan disks, fan shaft, compressor rotor and turbine rotor which are series connected by 3 spline joints (shown in Fig.7). The engine has four bearing supports. The engine is about 870mm long and the diameter is about 320mm. The maximum speed is 36,000rpm. Table 2 summarizes the material properties used in rotordynamic analysis.

**Table 2. Summary of material properties of the rotor**

| | Elastic modulus (GPa) | Density (Kg/m$^3$) | Poisson ratio |
|---|---|---|---|
| Fan disks, Compressor rotor | 100 | 4.44 E+03 | 0.34 |
| Fan shaft | 196 | 7.86E+03 | 0.3 |
| Turbine rotor | 193 | 8.16E+03 | 0.25 |

According to reference [4] and [10], an equivalent stiffness coefficient $\varepsilon_e$ is defined as follows:

$$\varepsilon_e = K_c \big/ K \tag{33}$$

where $K_c$ the real stiffness of joint structures, and $K$ is the stiffness of the reference axis segment. According to reference [10], the interval equivalent stiffness coefficients $\varepsilon_e$ of the three spline joints are summarized in Table 3 due to different assembly states. The stiffness of the first three supports is $1\times10^8\,N/m$, and the interval stiffness of support 4 which is close to turbine rotor is $[\,0.8\times10^8\,,1.0\times10^8\,]$ due to the uncertain temperature.

**Table 3. Summary of interval equivalent stiffness coefficients**

| | SJ-1 | SJ-2 | SJ-3 |
|---|---|---|---|
| $\varepsilon_e$ | [0.6-0.8] | [0.6-0.8] | [0.6-0.8] |

Fig.8 shows the Campbell diagram of the interval model, and the corresponding vibration modes are shown in Fig.6. It is seen from Fig.6 that the 1$^{st}$ mode is local mode of turbine rotor and the 2$^{nd}$ mode is the local mode of fan rotor. Table 4 summarizes the results of interval critical speeds.

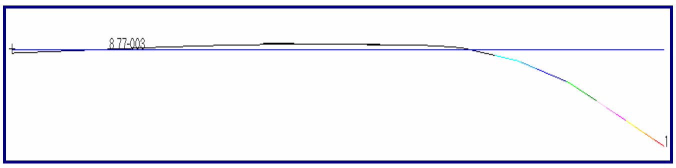

**a. Mode 1**

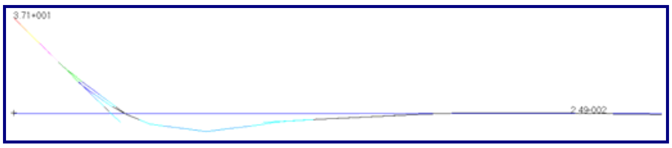

**b. Mode 2**

**Fig.6 Vibration modes of integral rotor**

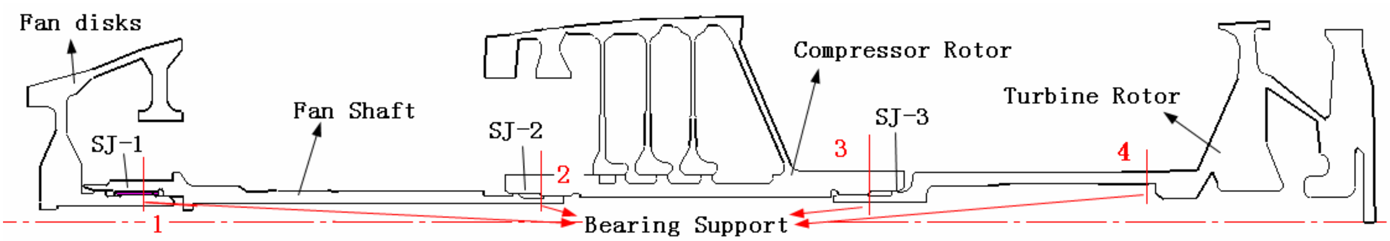

**Fig.7 Diagram of rotor structure**

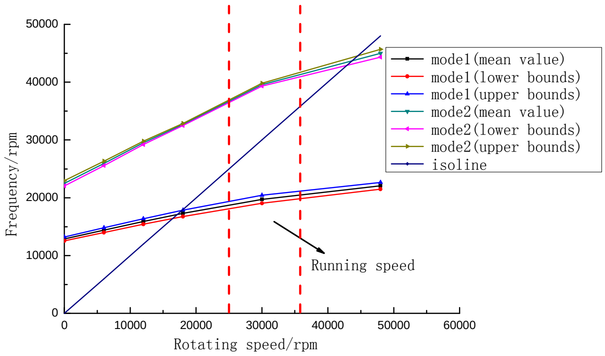


**Fig.8 Campbell diagram of interval model**

**Table 4. Summary of interval critical speeds**

| Mode | Interval critical speed (rpm) | Determined critical speed $\omega_c^C$ |
|---|---|---|
| 1 | [16400-17835] | 17118 |
| 2 | [42915-44575] | 43745 |

## 4.2 Analysis of test data

In order to validate the simulation analysis, an analysis of the test data including 8 trail runs is performed in this section. The time domain test data of the start up process of 7th test is taken for example. Fig.9 shows the time domain chart of the engine startup process, it can be seen that the vibration acceleration has three peaks in Area A, B and C. The frequency spectrums of the three areas are shown in Fig.10.

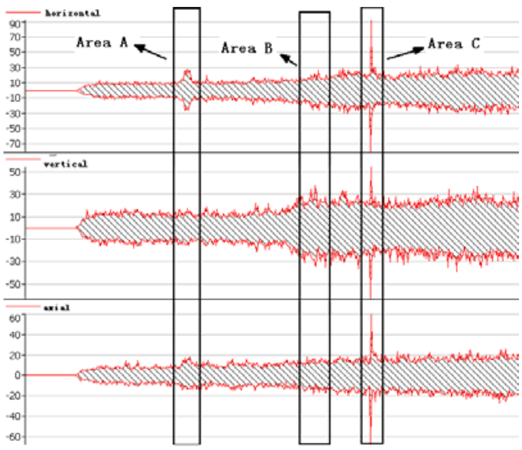


**Fig.9 The time domain chart of startup process**

From Fig.10 it can be seen that in Area A and C, the energy of rotating frequency is less than 15% of the total vibration energy, while high-frequency vibrations are much more than rotating frequency, thus the corresponding frequency in Area A and C are not the engine critical speeds.

The variation of vertical vibration acceleration of rotating frequency with rotating speed is shown in Fig.11. The 1st critical speed (288Hz, 17280rpm) can be captured from Fig.11.

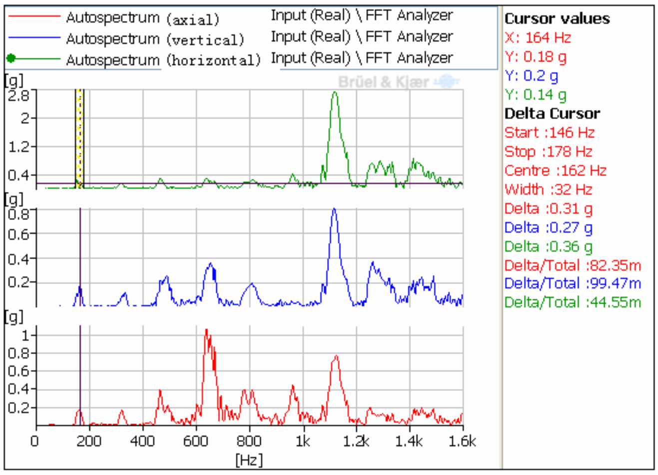


**a.** The frequency spectrum of area A

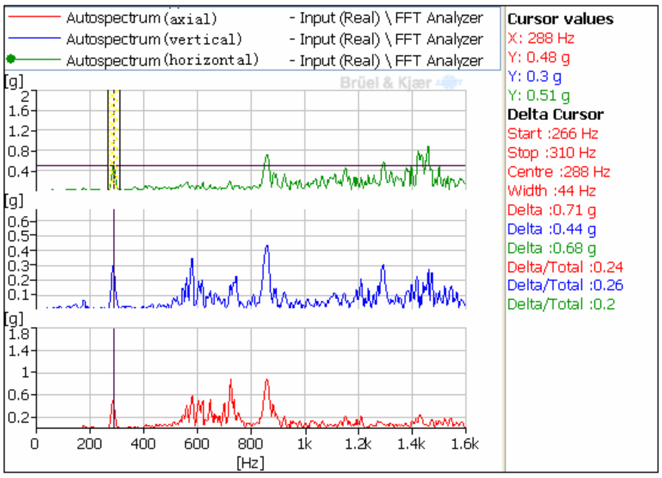


**b.** The frequency spectrum of area B

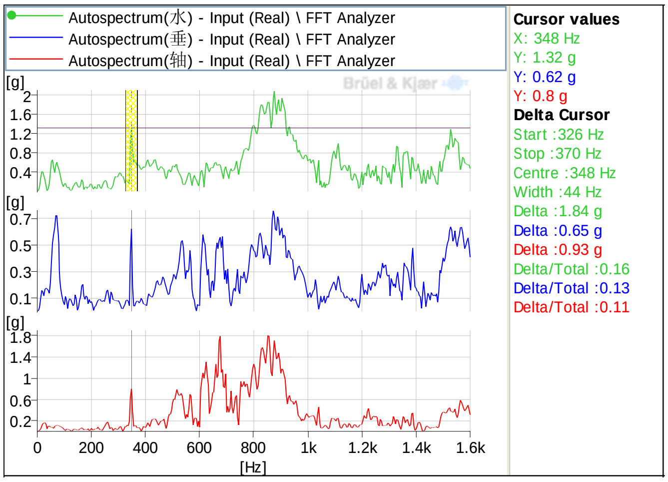


**c.** The frequency spectrum of area C

**Fig.10 The frequency spectrums**

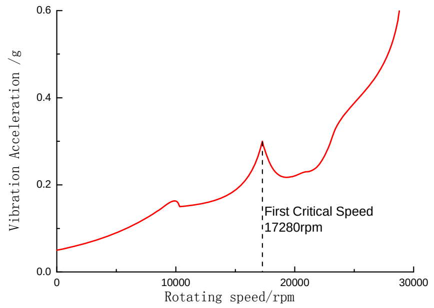


**Fig.11 Variation of vibration acceleration with rotating speed**

Table 5 summarizes the measured critical speeds of the eight tests. Only the first critical speed which is under the running speed is captured from the analysis of test data. Table 6 summarizes both predicted and measured interval critical speeds. It can be seen from Table 6 that the interval $1^{st}$ critical speed predicted by interval perturbation analysis is more close to the measured critical speed region compared with the critical speed yielded by determinated method which is the mean value shown in table). It is very necessary to calculate the rotordynamics with interval method, especially for aero-engines which lack samples and statistics characteristics.

**Table 5. Summary of measured $1^{st}$ critical speed**

| Test No. | Critical speed (rpm) | Test No. | Critical speed (rpm) |
|---|---|---|---|
| 1 | 16080 | 5 | 18000 |
| 2 | 17760 | 6 | 17040 |
| 3 | 18480 | 7 | 17280 |
| 4 | 16560 | 8 | 16180 |

**Table 6. Summary of predicted and measured critical speed**

| | Critical speed (rpm) | | Separation margin |
|---|---|---|---|
| | predicted | measured | |
| Upper bound | 17835 | [16080-18480] | 3.4% |
| Lower bound | 16400 | | 2.0% |
| Mean value | 17118 | | 7.4% |

The same engine was dismounted and assembled for 8 times, and the acceleration rates were kept at a same level in the eight start up process. To a great extent, these could make the critical speeds captured from test data more reliable even considering the effect of nonlinear response and the frequency estimation error. The uncertain critical speed is mainly caused by uncertain rotor stiffness and support stiffness due to different assembly conditions and different working loads. In the numerical analysis, only the interval uncertain connecting stiffness and stiffness of support 4 are considered, so the separation margin may be caused by other uncertain parameters such as stiffness of other supports.

## 5. CONCLUSIONS

If one views the uncertainty of the interval matrix as a perturbation around the midpoint of the interval matrix, one can solve the generalized interval eigenvalue problem by the perturbation method. By applying the interval extension to the matrix perturbation formulation, we present the interval perturbation approximating formula for estimating the upper and lower bounds on the set of all possible natural frequencies of the rotordynamic problem.

The present interval perturbation method is more accurate than determined method in rotordynamic analysis, and it is more efficient than probabilistic method such as Monte Carlo simulation (uniform distribution for the bounded uncertainty).

In this paper, only the effect of interval support stiffness and connecting structure stiffness on rotordynamics are studied, but how the assembly parameters such as fit clearance and preloads affect the stiffness is not included. The critical speeds are mainly monotonic to these stiffness parameters, but the effect of assembly parameters on stiffness is not monotonic [4]. The analysis of interval critical speeds with these assembly parameters would be presented in subsequent paper.

## 6. ACKNOWLEDGEMENTS

The paper is supported by Aeronautical Science Foundation of China (2009ZB51019).

## 7. REFERENCES

[1] Li Jianzhong,Yang Xiukuan, Huang Hongzhong, Feng Gang, Li Guodong, Research on fuzzy dynamic reliability design of single-rotor system. Journal of Dalian University of Technology, Vol. 43, No. 6 Nov. 2003, pp.768-770
[2]YaZhao Qiu, Singiresu S.Rao, A fuzzy approach for the analysis of unbalanced nonlinear rotor systems. Journal of sound and vibration, Vol.284, (2005), pp.299-323.
[3]Hongliang Yao, Qingkai Han, Bangchun Wen. THE APPLICATION OF FUZZY RANDOM FINITE ELEMENT METHOD ON ROTOR DYNAMICS[C], The 8th IFToMM International conference on Rotor Dynamics September 12-15, 2010, KIST, Seoul, Korea
[4]Liu Shuguo, Wang jun, Hong Jie, Zhang Dayi, Dynamics Design of the Aero-engine Rotor Joint Structures Based on Experimental and Numerical Study [C], Proceedings of ASME Turbo Expo 2010: Power for Land, Sea and Air, GT2010, June 14-18, 2010, Glasgow, Scotland
[5]Zhiping Qiu. Convex Method Based on Non-probabilistic Set-theory and its Application. Defense Industry Press, 2005, Beijing.
[6]Zhiping Qiu, Xiaojun Wang. Comparison of dynamic response of structures with uncertain-but-bounded Parameters using non-Probabilistic interval analysis method and Probabilistic approach [J]. International Journal of solids and Structures, 2003, 40: 5423-5439.
[7]Mc William S. Anti-optimization of uncertain structures using interval analysis [J]. Computers and Structures, 2001, 79: 421-430.
[8]Hu Xiaoyu, etc. Middle and Small Aeroengine Manual [M], Beijing: Aviation Industry Press, 2006.
[9]Hong Jie, Chen Meng, Ma Yanhong, Zhang Liming, Rotordynamic Analysis Method of Small Turbo-Fan Engine

Based on Finite Element Models[C], Proceedings of ASME Turbo Expo 2010: Power for Land, Sea and Air, GT2010, June 14-18, 2010, Glasgow, Scotland
[10]Li Junhui, 2009, A Study on Dynamics Design Method and Test of Aero-engine Rotor Joint Structures [D], Beijing: School of Jet Propulsion, Beijing University of Aeronautics and Astronautics.